The Annals of Statistics
1979, Vol. 7, No. 2, 237–257

AN ANALYSIS OF CELL MEMBRANE NOISE

BY STUART BEVAN[1], RICHARD KULLBERG[2] AND JOHN RICE[3]

The Salk Institute and University of California-San Diego

This paper describes an analysis of cell membrane noise. The physiological nature of cell membrane noise is outlined, and the experimental methods and data processing methods used are described. The statistical methods used to make inferences about interesting physiological parameters are discussed and a summary of some of the experimental findings is given. Since cell membrane noise is modelled as a form of shot noise, background material on shot noise is reviewed.

1. Introduction. During the last two years we have been involved in the investigation of the phenomenon known as cell membrane noise. This paper gives special attention to probabilistic and statistical aspects of this work, and both practical and theoretical problems that arose are discussed. We hope that this paper will serve as an interesting case study for the readers of *The Annals of Statistics*. In Section 2 we describe the physiological basis of cell membrane noise, and the experimental techniques and data processing methods we used. Section 3 contains a discussion of the statistical methods used to make inferences about certain physiological parameters. Section 4 gives a summary of some of the experimental findings. Since we have modelled cell membrane noise as a form of shot noise, an appendix contains a review of shot noise.

2. Membrane noise produced by acetylcholine. The transmission of signals from nerve to muscle involves the release of a transmitter chemical from the neuron which combines with receptor proteins on the muscle membrane. In the case of vertebrate skeletal muscles, the transmitter chemical is acetylcholine (ACh). The temporary combination of ACh with its receptor protein is believed to cause a conformational change in the protein, which in turn allows ions to flow through an associated ionic channel [2, 13]. During signal transmission a nerve cell releases sufficient amounts of ACh to cause the simultaneous opening of one to three hundred thousand channels. Minute currents (2–3 pA, 1 pA = 10^{-12} ampere) briefly flow through each of these channels, and the sum of these currents passing across the membrane resistance causes a depolarizing voltage change which, if sufficiently large, gives rise to an action potential and contraction of the muscle cell.

Using conventional intracellular recording techniques [12], it is relatively easy to record the electrical signal which is produced by the simultaneous opening of many

Received October 1977; revised June 1978.
[1]Supported by a Muscular Dystrophy Associations of America Fellowship.
[2]Supported by a Canadian MRC fellowship.
[3]Supported by a National Science Foundation grant. Correspondence concerning this paper should be addressed to Professor Rice.
AMS 1970 *subject classifications.* Primary 62P10; Secondary 60K99, 62M15.
Key words and phrases. Cell membrane noise, shot noise.

channels. Such signals range from a few millivolts to more than 50 mV, depending on experimental procedures. However, the signal produced by a single ionic channel cannot be seen in the intracellular recording. The change in membrane potential produced by the opening of a single channel is about 0.3 microvolt [13], whereas background noise is typically a few hundred microvolts (rms).

When a steady dose of ACh, small enough not to evoke an action potential, is artificially applied to the synaptic region, there is a very obvious increase in the amplitude of voltage fluctuations above the background noise level. These fluctuations are called cell membrane noise and are due to the random opening of ionic channels. The situation is similar to that of a vacuum tube in which the variability in numbers of electrons passing from cathode to plate gives rise to current noise. Time series methods may be used to analyze membrane noise, and estimates of basic channel properties such as conductance and duration of opening may be obtained [2, 13, 23].

Previous studies on membrane noise have characterized the ACh-activated channels found in amphibian [2, 13, 19] and avian muscle cells [16, 21]. The statistical models employed in those studies required that certain assumptions be made about individual channels. It was generally assumed that the channel conductance, γ, is fixed and that open times are random and exponentially distributed (with mean open time τ). It was also assumed that only a small fraction of the total number of channels is open at any given time and that the channels operate independently of each other. Thus the point process of opening times is approximately Poisson and the superposition of current flows through the individual channels forms a shot noise process of the kind discussed in the appendix (equation (5.4) and following). Recently, direct observation of single channel activity was made by means of isolating a small patch of membrane and reducing baseline recording noise [19]. This experiment substantiated some of the assumptions used in previous studies. It was shown that the waveform of channel opening is rectangular, and that the conductance of the channels is approximately constant. The marginal distribution of the number of open channels appeared Poisson.

Estimates of the channel conductance and mean channel open time have varied according to the kind of muscle studied. Values of channel conductance range from 15 to 60 pS(1 pS = 10^{-12} ohm^{-1}) in different species and mean channel open time varied from 2 to 10 msec (1 msec = 10^{-3} sec) at room temperature and normal cell resting potentials of -70 to -90 mV, (1 mV = 10^{-3} volts).

In our experiments, we chose to analyze the behavior of ACh-activated channels in mammalian tissue, in particular the tissue derived from skeletal muscle of rat embryos. In addition to obtaining a basic characterization of these channels, we also examined the effects of anti-receptor antibodies. It was previously observed that antibodies to ACh receptors can significantly reduce their response to ACh [5] and it seemed important to determine whether or not there was a partial impairment of channel function, since either a reduction in conductance or in open time would decrease the net effect produced by ACh.

Our experiments were conducted on isolated mammalian muscle cells which were grown in tissue culture. These cells are richly supplied with ACh receptors and their associated ionic channels. Normally, muscle cells grown in tissue culture are spindle or fiber shaped, but treatment with colchicine, which we routinely used, caused the cells to round up into small spheres in which it was easier to place electrodes. Using a low power microscope, cells about 50 to 100 microns in diameter were located and two microelectrodes were placed within each cell. By use of a technique known as "voltage clamping" the membrane potential was held at a fixed value (e.g., -70 mV) and the net current through ionic channels was measured.

The technique of voltage clamping required the use of two electrodes—one for recording the membrane potential and the second for supplying a current to hold the membrane potential steady. Any deviation from the desired membrane potential recorded by the first intracellular electrode was amplified, inverted, and fed back to the second electrode. This voltage applied to the second electrode produced a current which then passed across the membrane resistance, and by Ohm's law, produced a voltage which was in opposition to the original deviation. In this manner, the membrane voltage was kept constant. Normally, a change in membrane conductance produces a change in membrane voltage, but under voltage clamping, only the membrane current was allowed to change. Thus fluctuations in membrane conductance, due to the random opening of ionic channels, were recorded as fluctuations in the current passed through the second electrode. Current can pass across a cell membrane either through ionic channels or via membrane capacitance. However, current only flows through capacitance when the voltage across the capacitor changes. By holding the membrane voltage constant, one eliminates all current flow through the capacitor, leaving only current flow through ionic channels.

After placing two electrodes in a cell, the membrane potential was clamped at -60 or -70 mV. A control record of membrane noise was obtained. This baseline current noise was about .03 to .05 nA (rms) typically (1 nA = 10^{-9} amp). Only those cells were used which had a stable baseline current over a period of 1/2 minute or so. Following the control record, ACh was applied at a steady rate from a micro-pipette positioned near the surface of the cell and the membrane noise and mean current increased, due to the random opening and closing of channels. The rate of ACh delivery was adjusted to give a noise value of .10 to .15 nA (rms). It can be calculated that under this condition the average total number of channels open at any one time was about one to three thousand, giving rise to a mean current of 2 to 10 nA. The ACh was applied until the membrane current stabilized at a new mean value. After a suitable record was obtained, the ACh delivery was stopped and the membrane potential was allowed to return to baseline. The membrane potential was then clamped at a new value, and the experiment was repeated. Whenever possible, a cell was tested at membrane potentials ranging from -20 to -110 mV.

All data were recorded on analogue tape at 7 1/2 ips using a FM tape recorder. The membrane current was recorded simultaneously on two channels of the tape recorder. The input to one channel was bandpass filtered (.3 Hz to 3 kHz; 1 Hz = 1 cycle per second, 1 kHz = 1000 Hz) and amplified to fill the usable input range of the tape recorder. (A bandpass filter alters a signal by only allowing frequencies in a certain interval, or band, to "pass." Frequencies outside that band are suppressed.) This channel measured the fluctuations of the membrane current. The input to the second channel was used to record mean membrane current and therefore was not bandpass filtered.

In order to become familiar with the experimental techniques, the recording equipment, the data processing procedures, and the nature of the signal, some preliminary experiments were done and were analyzed over a wide frequency range (1 – 1000 Hz). From a pen recording of an entire experiment, stretches of the control run and of the ACh run which appeared qualitatively stationary were selected, low pass filtered at an appropriate frequency, and digitized. The spectrum of the control noise was seen to drop off roughly as f^{-1} in the low frequencies (1 – 50 Hz). From about 50 Hz on there was high frequency noise of increasing power, which was conjectured to be due to thermal noise in the electrodes and noise in the amplifier. Spikes in the spectrum at 60 Hz and its harmonics (120 Hz, 180 Hz, 240 Hz, · · ·) were also quite evident. The 60 Hz signal was an unwanted voltage picked up by the recording equipment from the main power lines. The ACh spectra had substantially more power in the low frequencies (1 – 2 orders of magnitude greater), so that the additional high frequency noise only became apparent above around 200 Hz. The spikes at 60 Hz, 120 Hz, 180 Hz, · · · were also evident. Fortunately, only the frequency range below 100 – 200 Hz was of interest, as will be seen, and since the analysis was carried out in the frequency domain, the 60 Hz component of the signal could easily be isolated.

As a check on the fidelity of the measurement system, white noise from a white noise generator was fed as a signal into the recording amplifiers. The frequency response was found to be flat over the range of interest.

After these initial investigations, data were processed in a uniform way. The channel containing the fluctuations was low pass filtered (cutoff 250 Hz) to avoid aliasing and digitized. (If a continuous signal is sampled at equi-spaced intervals, and the Fourier transform of the digitized record is computed, frequencies in the continuous signal that are faster than the sampling rate will be mistaken for slower frequencies in the digitized data. This phenomenon is known as "aliasing," and to avoid it the high frequencies are filtered out of the continuous signal prior to digitizing.) The digitizer only allowed certain combinations of record length, sample rate, and word length, and it was chosen to create records of length 1.96 sec. containing 4096 samples, each sample being recorded as a 12-bit word. This choice allowed us to obtain spectral estimates in the frequency range we desired. Since samples of ACh noise were typically 16 – 20 seconds long, 8 – 10 such records were produced per file. Segments of the series were lost in between

successive records, as the digitizer had no provision for temporarily holding them in a buffer. Files of control noise were typically 5 – 6 records long. The second channel, which was used to record the direct current flowing across the cell membrane, was digitized similarly.

To compute the spectrum from the high gain channel, the digitized data were decimated by a factor of two (i.e., every other sample was used to save computational time) giving a series $X(0), X(1), \cdots, X(2047)$ for each record. The periodogram was computed for each record as

$$I\left(\frac{k}{N}\right) = \frac{\Delta^2}{T}\left|\Sigma_{t=0}^{N-1}\exp\left(-\frac{2\pi ikt}{N}\right)X(t)\right|^2, \qquad k = 0, 1, \cdots, N-1 \tag{2.1}$$

where $T = 1.96$ sec, $\Delta =$ sampling interval ($= T/2048$) and $N = 2048$. The sum in (2.1) was computed by the fast Fourier transform algorithm [8]. The periodograms were then averaged over all the records in a file. The spectrum obtained from the control noise was subtracted from the spectrum of ACh noise, although this led to only a minor correction in the frequency band of interest. The computations were done on a CDC 3600 computer at the University of California at San Diego, and the spectra were recorded on tape and displayed on a Tektronix 4013 scope. When desired, permanent copies of the spectra were produced by a hard copy device attached to the scope or on a Calcomp plotter.

Illustrative traces of digitized records of control and ACh noise are shown in Figure 1, various power spectra are shown in Figures 2 and 5–8. The form of the fitted curve and the nature of the fitting method are discussed in the next section.

3. Statistical analysis. If a cell is clamped at a voltage v above the equilibrium potential, and a channel has conductance γ, then the current flow through an open channel is $v\gamma$. We let λ denote the average rate of channel openings. Assuming a channel is open a random length of time which is exponentially distributed with mean τ, then it is shown in the appendix (equation (5.4) and following) that the net current flow, $X(t)$, which is a shot noise process, has the first two moments

$$\mu = EX(t) = \lambda v\gamma\tau \tag{3.1}$$

$$\begin{aligned} c(u) &= \mathrm{Cov}(X(t), X(t+u)) \\ &= \lambda v^2\gamma^2\tau e^{-u/\tau} \\ &= \mu v\gamma e^{-u/\tau}. \end{aligned} \tag{3.2}$$

The power spectrum of $X(t)$ is thus

$$\begin{aligned} S(f) &= \int_{-\infty}^{\infty} e^{-2\pi ifu}c(u)du \\ &= \frac{2\mu v\gamma\tau}{1 + (2\pi f\tau)^2}. \end{aligned} \tag{3.3}$$

μ was estimated from the mean membrane current, and γ and τ were estimated by fitting the estimated power spectrum, obtained as described in the previous section.

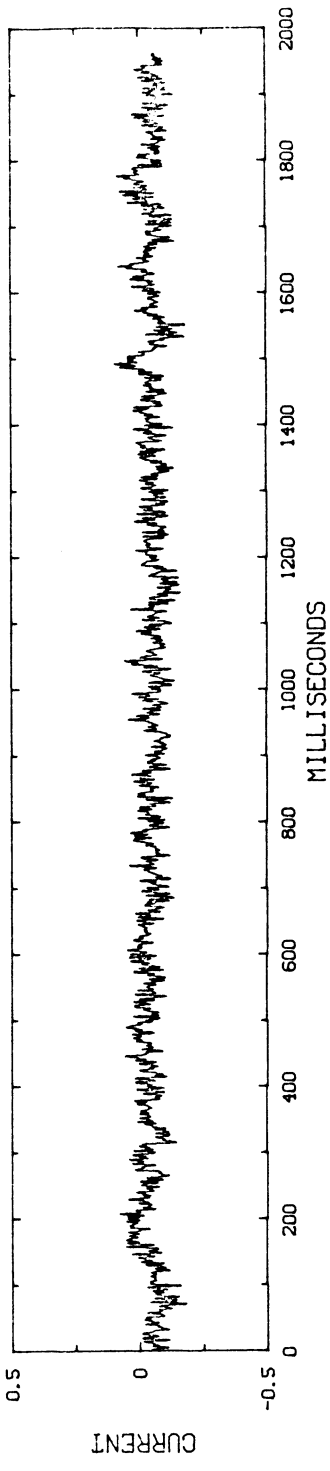

FIG. 1b. Traces of digitized records. ACh.

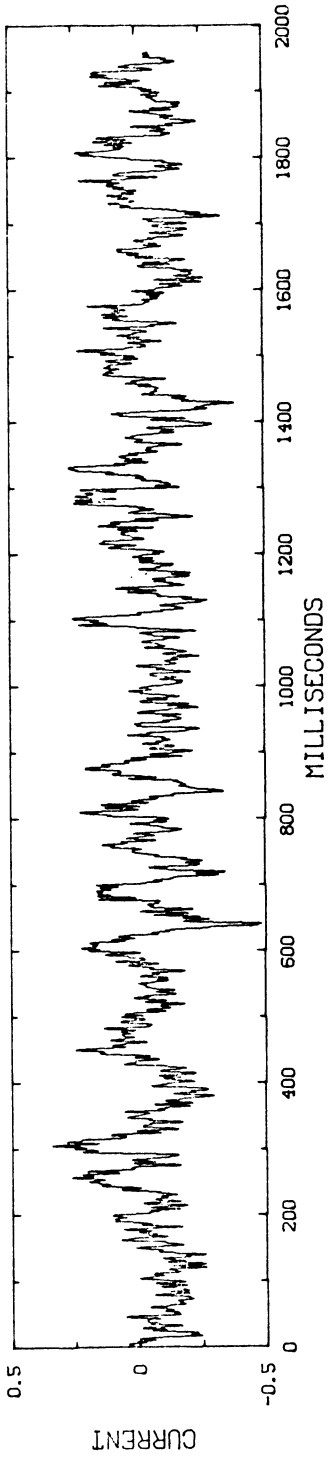

FIG. 1a. Traces of digitized records. Control.

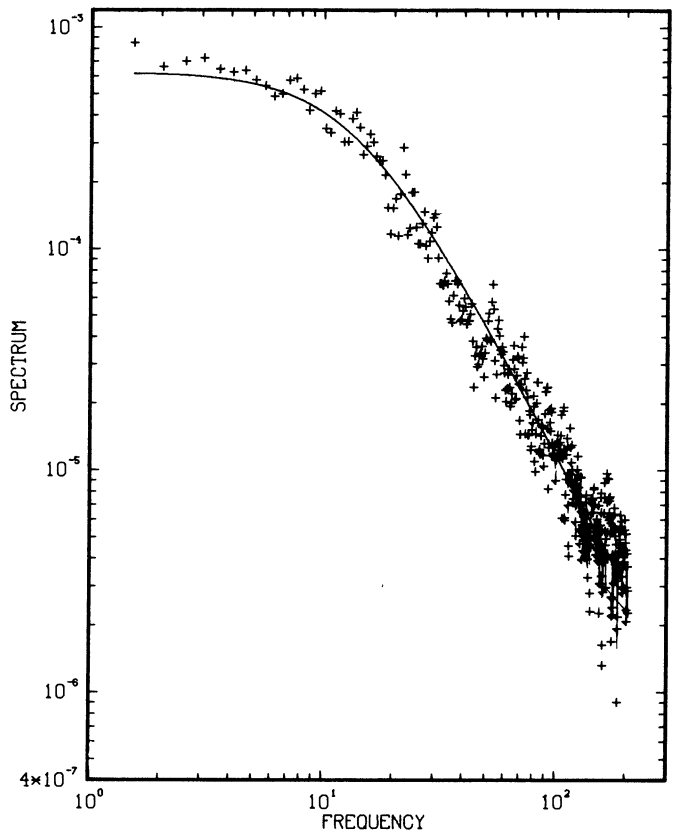

FIG. 2. A fitted spectrum with extra power in the low frequencies.

The fit was carried out over a frequency band ranging from .5 Hz to 100–200 Hz with narrow bands about 60 Hz and its harmonics deleted. The high frequency cutoff varied slightly from experiment to experiment, being determined by examining where the signal-to-noise ratio began to deteriorate substantially. (In Figure 2 increasing variability can be seen in the high frequency ranges.) The estimates of τ and γ are not too sensitive to the cutoff or to this additional variability.

Standard asymptotic theory for spectral estimates shows that the scaled periodogram ordinates at the frequencies given by the fast Fourier transform are approximately distributed as independent chi-square variates on 2 degrees of freedom [7]. If periodograms of successive records are averaged, as above, the resulting spectral estimates are therefore approximately distributed as independent gamma variates. Denoting the estimated spectrum by $\hat{S}(f_i)$, or simply $\hat{S}_i$, and the true spectrum by $S(f_i; \gamma, \tau)$ or S_i, where f_i ranges over a frequency domain of interest, writing down the approximate log likelihood and setting its derivatives equal to zero, one obtains the equations

$$\Sigma_{i=1}^{n} \frac{\hat{S}_i - S_i}{S_i^2} \frac{\partial S_i}{\partial \theta_k} = 0, \qquad k = 1, 2 \tag{3.4}$$

where $\theta = (\gamma, \tau)$. The solutions of these equations are, in some sense, asymptotic maximum likelihood estimates if the series is Gaussian and the fit is carried out over the entire spectrum, and if the series is not Gaussian the solutions can be viewed as approximate least squares estimates [24, 25, 26].

However, we used a different procedure to fit the spectrum. Estimates of τ and γ that minimized

$$\mathcal{S}(\gamma, \tau) = \Sigma_{i=1}^{n}\left[\log \hat{S}_i - \log S_i\right]^2 \tag{3.5}$$

were computed. This choice was made for several reasons: (1) a readily-available program for solving nonlinear least squares problems could be used; (2) the criterion being minimized, a distance in a familiar metric, had to us a more directly understandable objective meaning than did the approximate log likelihood; (3) it was not clear how sensitive the likelihood procedure was to different true underlying spectra or to the fact that the $\hat{S}_i$ were not precisely gamma distributed (because of the finite record length and because the estimated control spectrum had been subtracted); (4) the log transformation approximately stabilizes the variance [7]. If the model being fitted is correct, the two procedures are probably asymptotically equivalent, under reasonable conditions, as we will now indicate.

Minimizing $\mathcal{S}(\boldsymbol{\theta})$ involves solving the equations

$$\Sigma\left(\log \hat{S}_i - \log S_i\right)\frac{1}{S_i}\frac{\partial S_i}{\partial \theta_k} = 0. \tag{3.6}$$

Writing $\hat{S}_i = S_i + \delta_i$, this becomes

$$\Sigma \log(1 + \delta_i/S_i)\frac{1}{S_i}\frac{\partial S_i}{\partial \theta_k} = 0. \tag{3.7}$$

If several records are averaged, $\log(1 + (\delta_i/S_i) \simeq (\delta_i/S_i)$ and this equation is approximately the same as (3.4). It is interesting to observe that other methods are apparently approximately equivalent also; for example, note that

$$\begin{aligned} \mathcal{S}(\theta) &= \Sigma\left[\log\left(\hat{S}_i/S_i\right)\right]^2 \\ &= \Sigma\left[\log(1 + \delta_i/S_i)\right]^2 \\ &\simeq \Sigma(\delta_i/S_i)^2 \\ &= \Sigma\left[\frac{\hat{S}_i - S_i}{S_i}\right]^2 \end{aligned} \tag{3.8}$$

which leads to minimum χ^2 type estimates. The situation is thus somewhat analogous to that of equivalent B.A.N. estimators.

A crude analysis of the variability of the estimates can be made in a standard fashion via Taylor series expansions. Let $\hat{\theta}$ be the solution of the estimation equation which is of the form $\varphi(\theta) = 0$. Then

$$\varphi(\theta_0) \approx \varphi(\hat{\theta}) + A(\theta_0)\left(\theta_0 - \hat{\theta}\right) \tag{3.9}$$

where A is the differential of φ. Thus, if $A^{-1}(\theta_0)$ exists,

$$(\hat{\theta} - \theta_0) \approx -A^{-1}(\theta_0)\varphi(\theta_0). \tag{3.10}$$

Approximations to the mean and variance of $\hat{\theta}$ may be derived from (3.10) by using large sample properties of the periodogram. In our investigations the approximate standard errors of the estimates derived from a fit were computed but were not used extensively since the variation from cell to cell or from experiment to experiment was of more concern to us.

The nonlinear least squares equations for the estimates of γ and τ were solved numerically by an implementation of Marquardt's algorithm [17], which was used after attempts with Newton's method failed.

In the process of fitting spectra to experimental data, a problem arose, which was quite frustrating at the time, but which is, in retrospect, rather amusing. Many spectra, particularly those which were best resolved, were similar to that shown in Figure 3. For any one spectrum, one might shrug off such a shape as a random aberration, but upon seeing the same thing time and again, we became concerned that the apparent ripple in Figure 3 represented something real and unexpected. After considerable head scratching two possible explanations were conjectured: (1) extraneous spikes in the record, and (2) an echo. The former seemed the more likely, so traces of numerous digitized records were made, examinations of which showed nothing out of the ordinary. An echo seemed a possible explanation since if $x(t) = y(t) + \alpha y(t - s)$, then for small α, $\log S_x(f) \simeq \log S_Y(f) + 2\alpha \cos(2\pi fs)$. A visual examination of the spectra showed that the frequency of the ripple, s, was not constant, but decreased with increasing frequency, with $s \simeq .25$ sec initially, and that α was small and diminished at higher frequencies. It seemed rather unlikely that a physiological phenomenon would involve a time lag of this size, however. Plots of autocovariance functions showed nothing unusual. After some time in a state of quandary, we discovered that a peculiar kind of feedback process was apparently taking place: the signal from the cell went into the read head of the tape recorder, the tape then physically moved down from the read head to the write head (the transit time was $\frac{1}{8}$ sec.) and the signal from the write head was passed to the pen recorder which produced a version of the signal on a scroll of paper. The pen moved rather noisily on the paper, and the acoustic waves produced were picked up by the bath containing the cell and probably caused a variability in the capacitance between the bath and ground. This in turn produced a small current flow between bath and ground, which could not be discriminated from current flowing through the voltage clamp electrode. This process is very likely nonlinear (especially the air-water interface) which may explain the factor of 2 by which the transit time and the initial frequency of the ripple in the spectrum differ, as well as the variable rate of rippling across frequencies. No ripple was apparent in the spectra when the pen noise was eliminated.

We will conclude this section by discussing briefly why we went about the analysis in the way we did. We chose to work with the estimated power spectra of

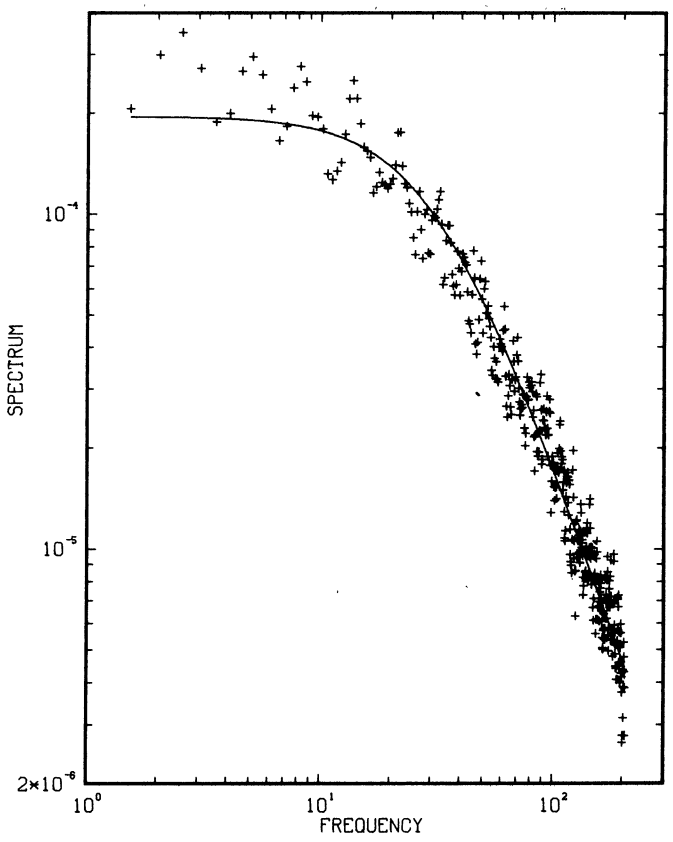

FIG. 3. A rippling spectrum.

the series for a number of reasons: (1) The series were qualitatively stationary. (2) Whether or not the model we used is reasonable, the power spectra are convenient descriptive statistics and can point out unsuspected problems, as happened in the case of the "echo." (3) The high frequency noise and the unwanted 60 Hz signal were easily isolated from the analysis—those frequency bands were simply ignored by the fitting procedure. If we had chosen to work with covariance functions, we would have had to employ some means of filtering out these frequencies. (4) Fitting the estimated spectra is a relatively simple and familiar procedure since the errors are approximately uncorrelated with each other. This also makes it easy to judge residuals. On the other hand, the successive ordinates of an estimated covariance function are correlated with each other, making it more difficult to judge residuals. (5) Since the series are nearly Gaussian, it must be fairly efficient to work with the first two moments of the data. (6) The fast Fourier transform algorithm makes it possible to perform the calculations quite economically. For shot noise driven by a relatively slow Poisson process alternative methods might well be preferable, and it

would be interesting to see such methods developed. It would also be interesting to consider the estimation problem when the Poisson process is not stationary, but perhaps changes slowly in time.

We will be happy to make samples of the data available to any reader interested in trying alternative methods of analysis. The data is on magnetic tape in 12-bit words. In order to process the data a reader would have to "unpack" the 12-bit words for use on his computer.

4. Conclusions. We now will indicate very briefly some of the results of various series of experiments on cultured rat cells. More details will be published elsewhere.

(i) *Spectral shape.* As illustrated in Figures 2 and 5–8 the equation (3.3) was a reasonable fit to the power spectra. As in Figure 2 however, extra power in the low frequencies was noticed in many spectra. Several possible explanations were entertained: (1) minute contractions of the cell in the presence of ACh might produce such deviations; however, no contractions were observed, and the contractility of the cells was minimized due to colchicine treatment; (2) slow fluctuations in the rate of ACh delivery would make the rate of the point process of opening times variable and would therefore produce this extra power. Precautions were taken to prevent this, however, such as keeping the pipette a long distance (25–50 mm) from the cell and using a constant current apparatus to deliver the ACh; (3) the length of the channel open time, instead of being exponentially distributed, might have slightly heavier tail; (4) there might be a lack of independence between channels or some form of clustering of open times—e.g., if a ACh molecule skipped from receptor to receptor, as proposed by Katz and Miledi [14]. Point processes with such clustering have been considered in the literature, and an expression for the power spectrum of the resulting shot noise process can be derived [20].

(ii) *Voltage dependence.* The channel conductance of the cells was found to depend linearly on membrane potential over a range of -30 to -110 mV becoming smaller with increasing negativity. The mean conductances at -40, -70, -90 mV were 47 ± 8 pS($n = 19$), 42 ± 9 pS($n = 20$), 38 ± 7 pS($n = 12$), respectively.

The channel open time was related exponentially to membrane potential as $\tau = A \exp(-BV)$; an example is shown in Figure 4. Mean values of A and B were 3.1 msec and .013 mV^{-1}. This corresponds to a mean open time of 7.7 msec at -70 mV. It has been proposed [2] that the effect of membrane potential on channel open time is due to the interaction of the dipole moment of the gating molecule and the electric field in the cell membrane.

(iii) *Temperature dependence.* Temperature studies were carried out over a range of $8 - 37°C$ and it was found that conductance increased linearly with temperature. Channel open time was found to become smaller with increasing temperature. Figures $5 - 8$ show the dependence of τ on membrane potential quite clearly.

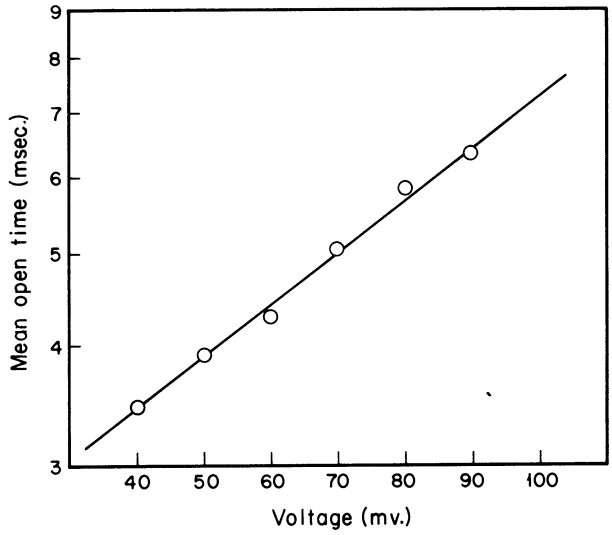

FIG. 4. Dependence of mean open time on voltage.

According to the Arrhenius equation [9]

$$\alpha = Ce^{-e_A/RT} \tag{4.1}$$

where $\alpha = (1/\tau)$ = rate constant for channel closing, C = constant (frequency factor), e_A = activation energy, R = gas constant, and T = absolute temperature. Plotting log α vs. $1/T$ gave a linear relationship (Figure 9) in agreement with this equation. Estimates of γ and τ are not well resolved when a spectrum such as that shown in Figure 5 is fitted, and the agreement of the estimate of τ with the Arrhenius equation at such extremes gives more confidence in the estimates. The activation energy was estimated as 20.8 ± 2.6 kcal/mol from 5 cells. From the frequency factor, which had a median value of 2.3×10^{29}/sec, the entropy of activation [8] can be calculated to be 73.7 cal/deg mol, which suggests that there is a substantial increase in rotational and vibrational freedom of the gating molecule in the transition state between open and closed conformation. This entropy change offsets the relatively large activation energy and thereby increases the rate constant. If there were no entropic change, the frequency factor would be 1.7×10^{13}/sec at room temperature and the channel would remain open for about 2 minutes.

(iv) *Myasthenic serum.* Human patients with myasthenia gravis have antibodies against ACh receptors in their sera. These antibodies bind to ACh receptors and cause a great reduction in muscle sensitivity to ACh [5, 6]. In principle, this reduction could be explained in several ways: (1) there could be a biological degradation of receptors, totally eliminating them from the cell surface; (2) there

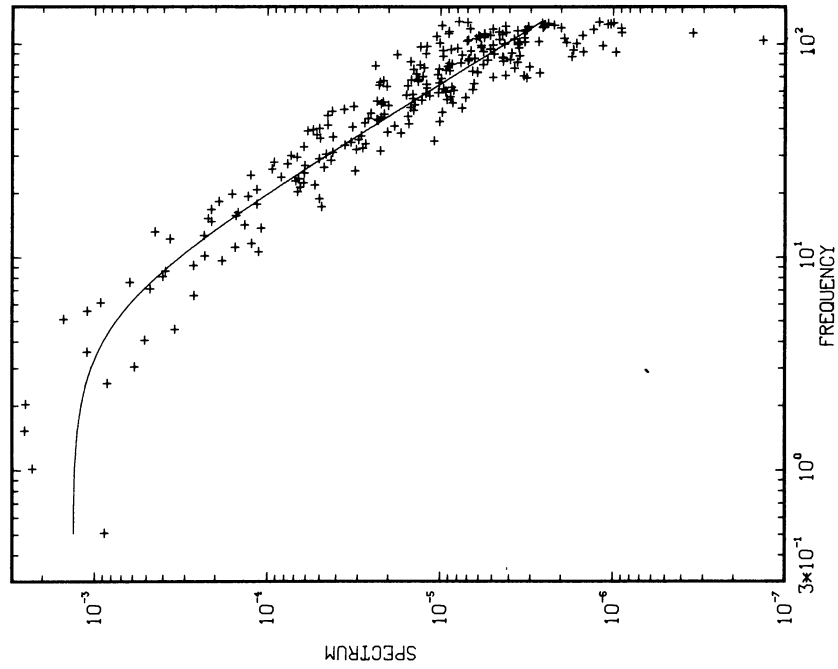

FIG. 6. Spectrum of a cell at 18°. τ = 28.4 msec.

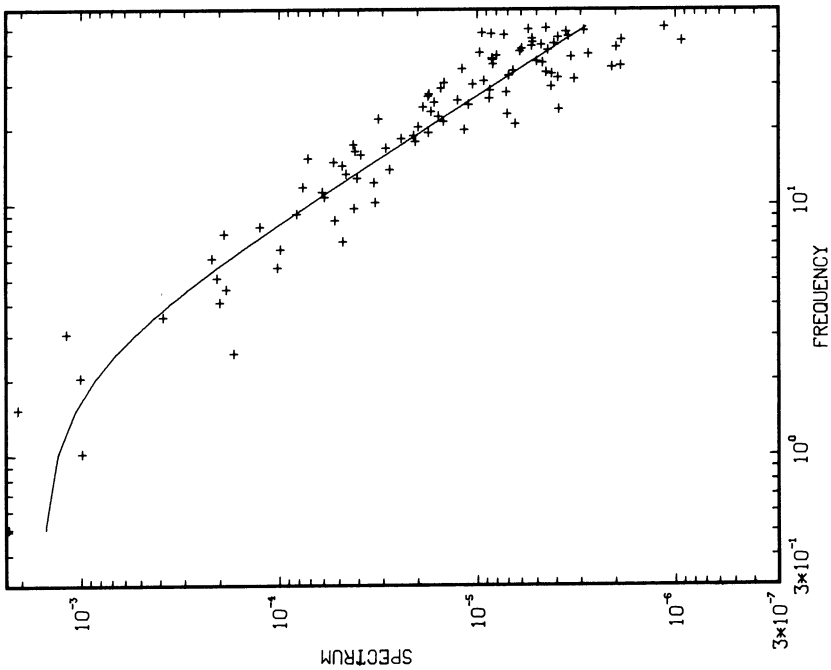

FIG. 5. Spectrum of a cell at 12°. τ = 74.3 msec.

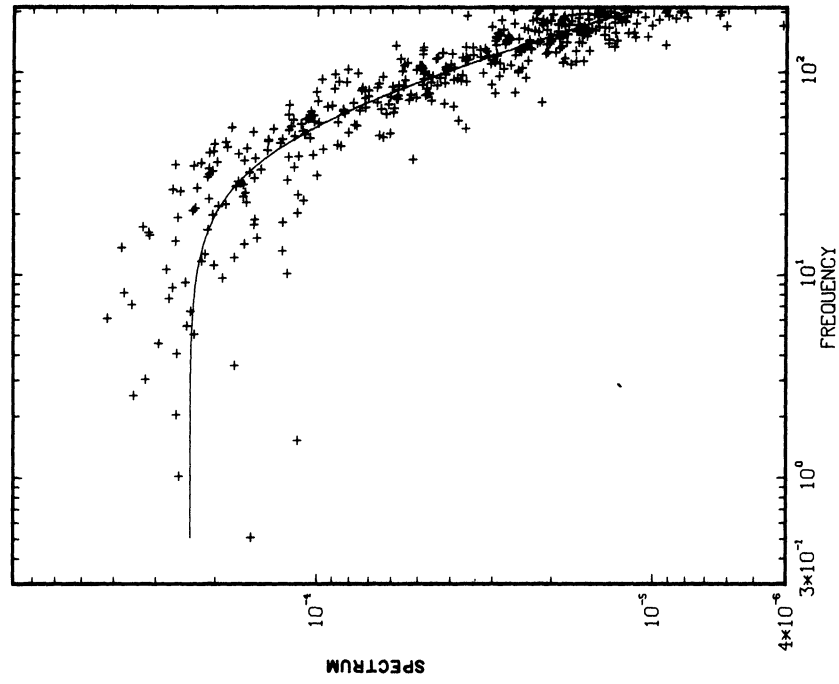

FIG. 8. Spectrum of a cell at 33°. τ = 3.5 msec.

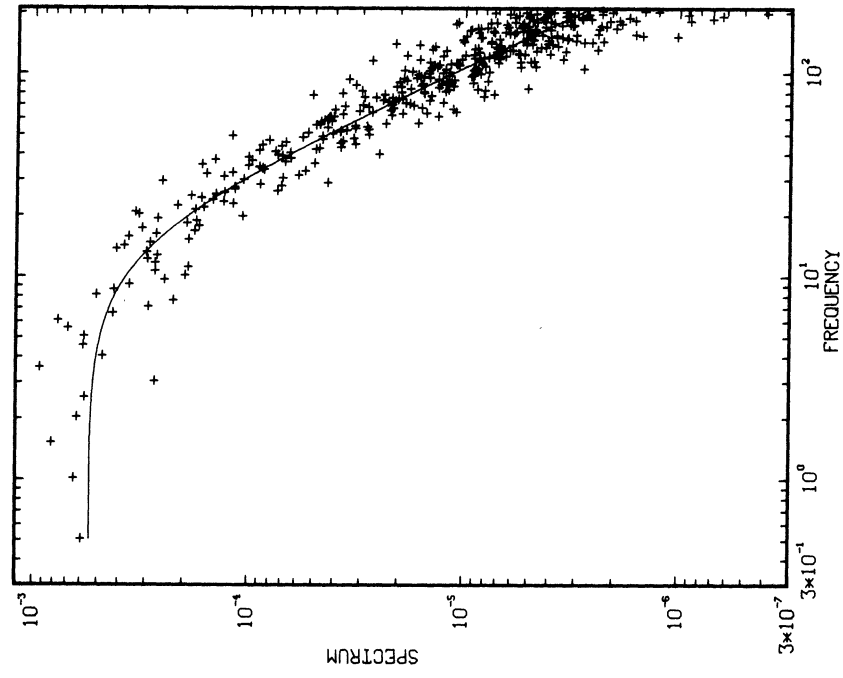

FIG. 7. Spectrum of a cell at 24.5° τ = 10.9 msec.

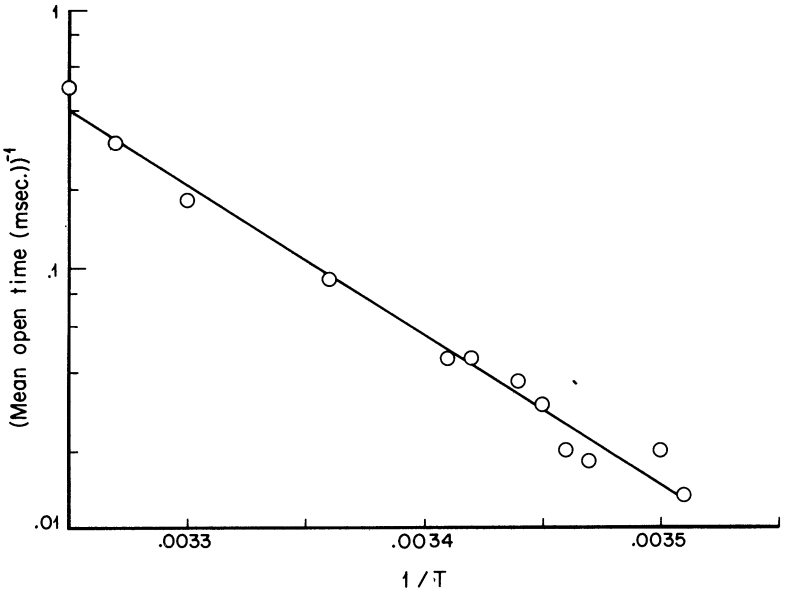

FIG. 9. An Arrhenius plot showing dependence of open time on temperature.

could be a complete block of receptor function, without degradation, analogous to the effect of curare; (3) there could be a partial impairment of channel function, either a reduction in τ or γ or both. Experiments were performed to determine the mechanism by which antibody against the ACh receptor reduces muscle sensitivity to ACh. It was found that the antibodies increased approximately sixfold the rate of degradation of ACh receptor on cultured rat muscle tissue, resulting in a lowered density of ACh receptors. Also, spectral analysis demonstrated that those ACh receptors which remained functional had a small impairment in function. The mean charge passed through a channel during a single opening was reduced by about 30% [11]. Both γ and τ were reduced by binding of antibody.

The preceding analysis has been based on the second-order structure of the shot noise process, and since the model described in Section 2 yields simple expressions for moment functions of all orders, it is natural to try to use higher-order moments of the data to check on the validity of the model, or perhaps to discriminate between models. Also, it is clear that additional information about the parameters is contained in higher-order moments; however, it is not clear how this information could best be incorporated.

The sample mean, variance, skewness, and kurtosis were computed for each record in a file, and their standard deviations were calculated. From (5.5) it can be

seen that the shot noise model gives the standardized skewness of the marginal distributions as $(8V\gamma/9\mu)^{\frac{1}{2}}$ and the standardized kurtosis as $V\gamma/\mu$. $V\gamma/\mu$ is the proportion of the mean current due to a single channel. It was consistently observed that the estimated skewness and kurtosis were very small, and that their standard errors were of the same as, or of larger order of magnitude than, the estimates. The third order cumulant function $c(t_1, t_2)$ was similarly estimated for

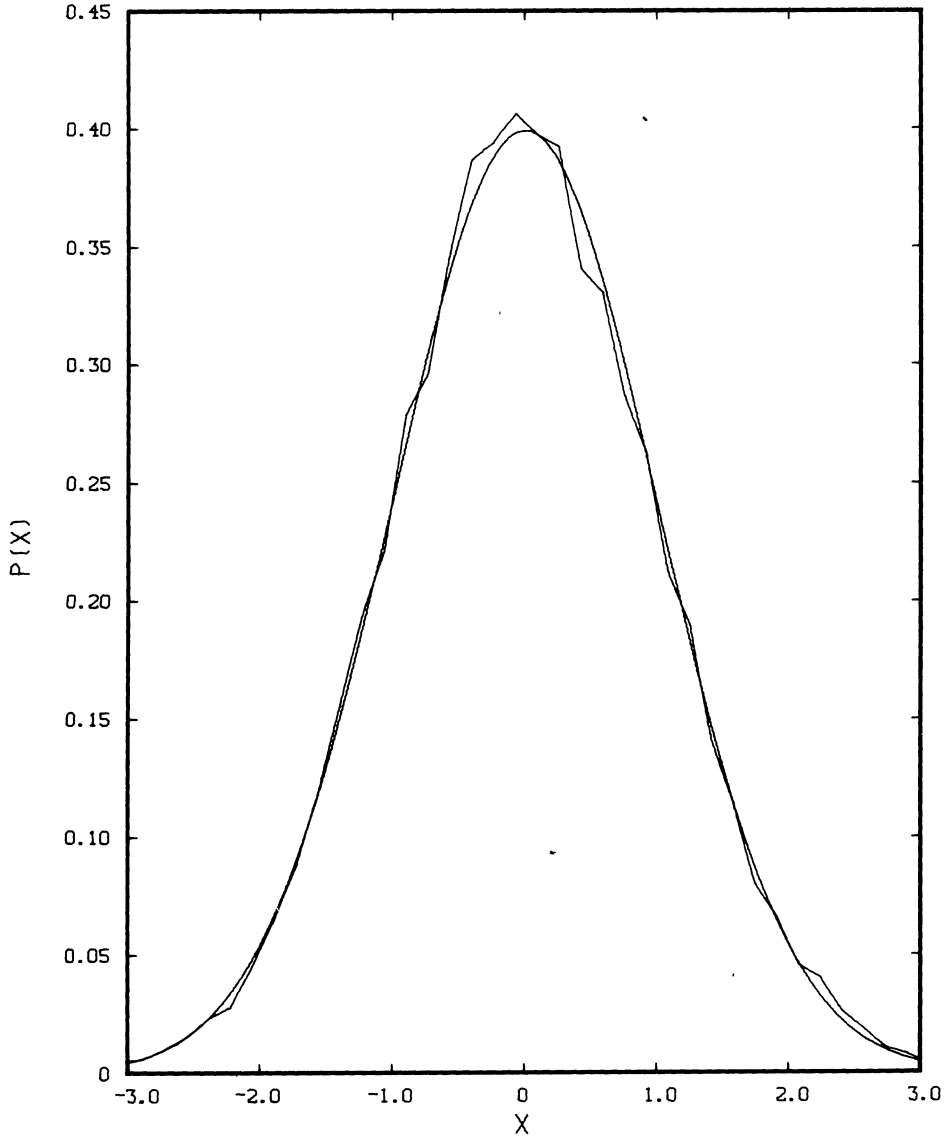

FIG. 10. A smoothed histogram and a fitted Gaussian density. (n = 49,152).

several experiments over a small grid (t_1, t_2) and again the estimates were so small as to be indistinguishable from zero.

Histograms were computed for several experiments, and these all appeared quite close to Gaussian (Figure 10). In many cases there was a slight suggestion of positive skewness (which is consistent with the model), but this was not consistently observed. The nearly Gaussian character of the data is to be expected in light of the well-known convergence of shot noise processes to Gaussian processes [20]. As noted in Section 3, in a typical experiment an average of $1000 - 3000$ channels were open at any given time.

The histograms were quickly computed by counting the number of observations in a file that fell at each of the discrete levels of the digitizer. Adjacent cells were pooled to smooth the final histogram and improve its rèsolution. Out of curiosity we displayed some unsmoothed histograms obtaining results like that in Figure 11. Although we expected the variability to increase, we did not expect the oscillatory character shown in the figure. Examination showed that the oscillations were larger than would be expected on the basis of the standard errors of the counts and that they had a systematic character. Further investigation showed that there were peculiar nonuniformities in the digitizer; for example, even bits turned on too often and odd bits too seldom.

Examination of equation (5.6) suggests that it might be of interest to estimate the characteristic function $\varphi(\omega)$ of the marginal distribution. Since the signal recorded during the application of ACh is the sum of the shot noise and the background or control noise, which we assume independent, and since recordings were also made of the control noise alone, it is natural to estimate the ratio of the corresponding characteristic functions. Because of the form of equation (5.6) we first tried to estimate $\log \varphi(\omega)$ and made the empirical discovery that the estimate $\log \hat{\varphi}(\omega)$, where

$$\hat{\varphi}(\omega) = \int e^{i\omega x} dF_n(x), \tag{4.2}$$

is badly biased. In retrospect it was clear why this was so. Note that $\log \hat{\varphi}(\omega) = \frac{1}{2}\arg[\hat{\varphi}(\omega)] \log|\hat{\varphi}(\omega)|^2$. $|\hat{\varphi}(\omega)|^2$ itself is biased since, in the case that $\hat{\varphi}(\omega)$ has been estimated from n independent observations,

$$\begin{aligned} E|\hat{\varphi}(\omega)|^2 &= |\varphi(\omega)|^2 + \operatorname{Cov}[\hat{\varphi}(\omega), \overline{\hat{\varphi}(\omega)}] \\ &= \frac{n-1}{n}|\varphi(\omega)|^2 + \frac{1}{n} \end{aligned} \tag{4.3}$$

as can be easily calculated [10]. The inverse tangent and logarithmic transformations lead to additional bias. For this reason we merely estimated the real and imaginary parts of $\varphi(\omega)$. It is to be expected that the ratio of two sample characteristic functions does not behave very well, especially for large ω, with respect to both bias and variance, and indeed this was true. Since in our case we were trying to detect very small deviations from a Gaussian shape, it appeared that

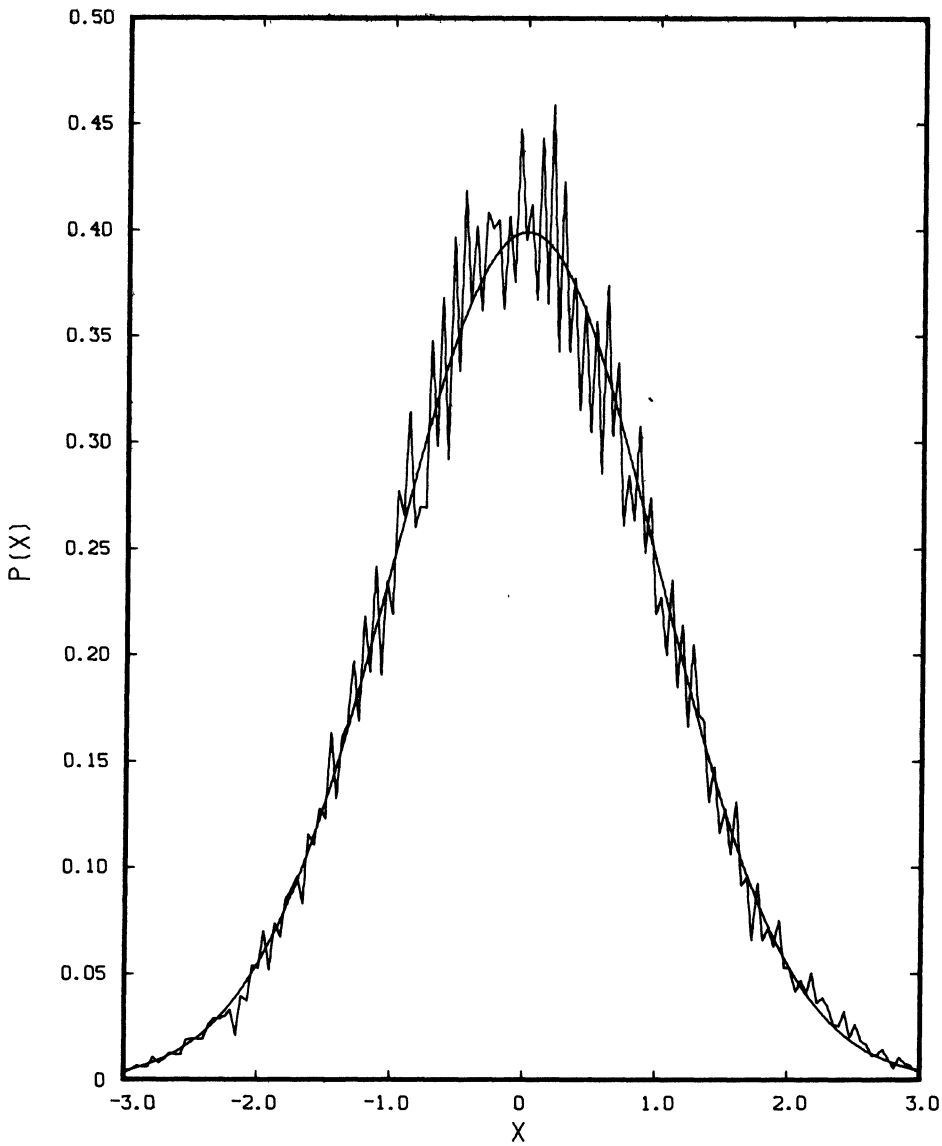

FIG. 11. The same histogram unsmoothed and suspiciously spiky.

we could not gain any reliable information, especially in light of the peculiarities of the digitizer. Parenthetically, we might note that sample characteristic functions are deceptively smooth, due to the high correlation of different points along the curve [10]. Thus just as one feels more comfortable working with a sample spectral density than a sample covariance function because of the simple statistical behavior of the former, one feels more comfortable working with an estimated probability density function than with a sample characteristic function.

5. Appendix on shot noise. In this appendix some properties of shot noise are reviewed; more details can be found in [20]. Shot noise is a stochastic process formed in the following way: events occur at times τ_i given by the realization of a stochastic point process N. At each such time there is a realization of a possibly random function g, the "shot effect"; these realizations are assumed to be independent of each other and of the process N. The shot noise process $X(t)$ is the superposition of the shot effects

$$X(t) = \Sigma g(t - \tau_i) = \int g(t - u)dN(u). \tag{5.1}$$

Shot noise models have been used in many scientific areas, including electronics, acoustics, optics, and biophysics.

Expressions for the moment functions of a shot noise process driven by a general point process N may be derived [20]. If N is Poisson with rate λ, the k^{th} order cumulant function and cumulant spectrum are

$$C_x(t_1, \ldots, t_k) = \lambda \int E\Pi_j g(t_j - u)du \tag{5.2}$$

$$S_x(f_1, \ldots, f_k) = \lambda E[G(f_1) \cdots G(f_k)] \tag{5.3}$$

where $\Sigma f_j = 0$, and S_x and G are the Fourier transforms of C_x and g.

A shot noise process that is of interest in previous sections consists of N stationary Poisson and

$$g(t) = \begin{cases} = \gamma & \text{if } 0 \leqslant t \leqslant T \\ = 0 & \text{otherwise} \end{cases} \tag{5.4}$$

where $P(T > t) = e^{-\alpha t}$.

(If $\gamma = 1$, $X(t)$ is the number of customers in a $M/M/\infty$ queue.) The k^{th} order cumulant function is found to be

$$\begin{aligned} c(t_1, \cdots, t_k) &= \lambda \int E\Pi_j g(t_j - u)du \\ &= \lambda \gamma^k \int_{-\infty}^{t_{\min}} P(T \geqslant t_{\max} - u)du \\ &= \frac{\lambda \gamma^k}{\alpha} \exp[-\alpha(t_{\max} - t_{\min})] \end{aligned} \tag{5.5}$$

where

$$t_{\max} = \max(t_1, \ldots, t_k)$$
$$t_{\min} = \min(t_1, \ldots, t_k).$$

A similar calculation gives the marginal characteristic function as

$$\log \psi(\omega) = \frac{\lambda}{\alpha}[\cos(\omega\gamma) - 1] + i\frac{\lambda}{\alpha}\sin(\omega\gamma), \tag{5.6}$$

so that $X(t)$ is a scaled Poisson random variable.

It is interesting to compare this process to a process with deterministic shot effect $g(t) = \gamma \exp(-\alpha t)$. The k^{th} order cumulant function and the marginal characteristic function of this process can be calculated to be

$$c(t_1, \ldots, t_k) = \frac{\lambda \gamma^k}{k\alpha} \exp\left[-\alpha \Sigma (t_j - t_{\min})\right], \tag{5.7}$$

$$\log \psi(\omega) = \frac{\lambda}{\alpha} \int_0^{\gamma\omega} \frac{\cos t - 1}{t}\, dt + i \frac{\lambda}{\alpha} \int_0^{\gamma\omega} \frac{\sin t}{t}\, dt. \tag{5.8}$$

The cumulant functions of the two processes differ in shape for $k > 2$, and the characteristic functions can be compared by expanding them. k^{th} order cumulants, which are the coefficients of $(i\omega)^k/k!$ in the series, differ by a factor of k. If λ/α is large, both standardized processes are approximately Gaussian having k^{th} order cumulants of order $(\lambda/\alpha)^{1-k/2}$ [20]. For the first process discussed λ/α is the average number of shot effects contributing to $X(t)$.

Acknowledgments. We thank Dr. Ken Helland for generously giving technical advice about the use of the digitizer and the CDC3600. Professors Richard Olshen and Murray Rosenblatt and the editorial staff of the *Annals of Statistics* made comments which improved the readability of the paper.

REFERENCES

[1] ABRAMOWITZ, M. and STEGUN, I. (1970). *Handbook of Mathematical Functions*. Dover, New York.
[2] ANDERSON, C. R. and STEVENS, C. F. (1973). Voltage clamp analysis of acetylcholine produced end-plate fluctuations at frog neuromuscular junction. *J. Physiol.* **235** 655–691.
[3] BARTLETT, M. S. (1955). *Introduction to Stochastic Processes*. Cambridge Univ. Press.
[4] BARTLETT, M. S. and KENDALL, D. G. (1946). The statistical analysis of variance–heterogeneity and the logarithmic transformation. Supplement to the *J. Roy. Statist. Soc.* **8** 128–133.
[5] BEVAN, S., HEINEMANN, S. F., LENNON, V. A. and LINDSTROM, J. (1976). Reduced muscle acetylcholine sensitivity in rats immunized with acetylcholine receptor. *Nature* **260** 438–439.
[6] BEVAN, S., KULLBERG, R. and HEINEMANN, S. F. (1977). Human myasthenic sera reduce acetylcholine sensitivity of human muscle cells in tissue culture. *Nature* **267** 263–265.
[7] BRILLINGER, D. R. (1975). *Time Series: Data Analysis and Theory*. Holt, Rinehart and Winston, New York.
[8] COOLEY, J. W. LEWIS, P. A. W. and WELCH, P. D. (1976). The fast Fourier transform and its application to time series analysis. In *Statistical Methods for Digital Computers: Mathematical Methods for Digital Computers*, V3 (Enslein et al., eds.). Wiley Interscience, New York.
[9] DANIELS, F. and ALBERTY, R. A. (1975). *Physical Chemistry*. Wiley, New York.
[10] FEUERVERGER, A. and MUREIKA, R. (1977). The empirical characteristic function and its applications. *Ann. Statist.* **5** 88–97.
[11] HEINEMANN, S., BEVAN, S., KULLBERG, R., LINDSTROM, J. and RICE, J. (1977). Modulation of the acetylcholine receptor by anti-body against the receptor. *Proc. Nat. Acad. Sci.* **74** 3090–3094.
[12] KATZ, B. (1966). *Nerve, Muscle, and Synapse*. McGraw-Hill, New York.
[13] KATZ, B. and MILEDI, R. (1972). The statistical nature of the acetylcholine potential and its molecular components. *J. Physiol.* **224** 665–699.
[14] KATZ, B. and MILEDI, (1973). The binding of acetylcholine to receptors and its removal from the synaptic cleft. *J. Physiol.* **231** 549–574.
[15] KATZ, B. and MILEDI, R. (1973). The characteristics of "end-plate noise" produced by different depolarizing drugs. *J. Physiol.* **230** 707–717.
[16] LASS, Y. and FISCHBACH, G. D. (1976). A discontinuous relationship between the acetylcholine activated channel conductance and temperature. *Nature* **263** 150–151.

[17] MARQUARDT, D. W. (1963). An algorithm for least squares estimation of non-linear parameters. *SIAM J.* **11** 431–441.
[18] NEHER, E. and SAKMANN, B. (1976). Noise analysis of drug induced voltage clamp currents in denervated frog muscle fibers. *J. Physiol.* **258** 705–729.
[19] NEHER, E. and SAKMAN, B. (1976). Single-channel currents recorded from membrane of denervated frog muscle fibers. *J. Physiol.* **258** 705–729.
[20] RICE, J. (1977). On generalized shot noise. *Advances in Appl. Probability* **9** 553–565.
[21] SACHS, F. and LECAR, H. (1973). Acetylcholine noise in tissue culture muscle cells. *Nature New Biology* **246** 214–216.
[22] VALE, W. and GRANT, B. (1975). *Methods in Enzymology*, Vol. XXXVII, Hormone Action, Part B, Peptide Hormones. Exford Academic Press, 82–93.
[23] VERVEEN, A. and DEFELICE, L. (1974). Membrane noise. *Progr. Biophys. Mol. Biol.* **28** 189–265.
[24] WALKER, A. M. (1964). Asymptotic properties of least-squares estimates of parameters of the spectrum of stationary non-deterministic time-series. *J. Austral. Math. Soc.* **4** 363–384.
[25] WHITTLE, P. (1953). Estimation and information in stationary time series. *Ark. Math.* **2** 423–434.
[26] WHITTLE, P. (1962). Gaussian estimation in stationary time series. *Bull. Inst. Internat. Statist.* **39** 105–129.

STUART BEVAN AND RICHARD KULLBERG
THE SALK INSTITUTE
SAN DIEGO, CALIFORNIA 92112

JOHN RICE
DEPARTMENT OF MATHEMATICS
UNIVERSITY OF CALIFORNIA-SAN DIEGO
LA JOLLA, CALIFORNIA 92093